

Projection of two biphoton qutrits onto a maximally entangled state

A. Halevy, E. Megidish, T. Shacham, L. Dovrat, and H. S. Eisenberg

Racah Institute of Physics, Hebrew University of Jerusalem, Jerusalem 91904, Israel

Bell state measurements, in which two quantum bits are projected onto a maximally entangled state, are an essential component of quantum information science. We propose and experimentally demonstrate the projection of two quantum systems with three states (qutrits) onto a generalized maximally entangled state. Each qutrit is represented by the polarization of a pair of indistinguishable photons - a biphoton. The projection is a joint measurement on both biphotons using standard linear optics elements. This demonstration enables the realization of quantum information protocols with qutrits, such as teleportation and entanglement swapping.

PACS numbers: 03.67.Bg, 42.50.Dv

Quantum entanglement is a basic resource for quantum information communication and processing protocols. It can be achieved either by certain physical interactions between two quantum systems [1] or by a projection of both systems with a specific measurement [2]. The projection of two independent quantum states onto a maximally entangled state destroys them. Nevertheless, such a projection is required for the implementation of innovative quantum information protocols, such as quantum teleportation [3, 4] and entanglement swapping [5], which can be used to realize quantum repeaters [6].

Quantum information is often encoded in the polarization of photons. It is possible to realize a three-level quantum system, a qutrit, by the polarization of a pair of photons [7]. If the two photons are indistinguishable in any degree of freedom except for their polarization, they occupy the three-dimensional symmetric triplet subspace of the Hilbert space of two qubits. Such a general biphoton state can be written as:

$$|\psi_{bi}\rangle = (\alpha_0 \frac{a_h^{\dagger 2}}{\sqrt{2}} + \alpha_1 a_h^{\dagger} a_v^{\dagger} + \alpha_2 \frac{a_v^{\dagger 2}}{\sqrt{2}}) |\text{vac}\rangle, \quad (1)$$

where a_h^{\dagger} (a_v^{\dagger}) is the creation operator of a horizontally (vertically) polarized single photon in the spatial mode a , α_0 , α_1 , and α_2 are the amplitudes of the three biphoton states, and $|\text{vac}\rangle$ is the vacuum state. Using linear optical elements limits the possible rotations of biphoton qutrits [8]. Nevertheless, adding ancilla photons increases the amount of accessible rotations [9]. Qutrits have also been realized by superimposing a single photon between three orbital momentum [10, 11], spatial [12], and temporal [13] modes. Arbitrary rotations can be applied to such qutrit realizations [14], and there is even a suggestion for a conversion technique between biphotons and single photons in three modes [15]. The incorporation of qutrits can also enhance the performance of quantum communication protocols [16–19]. Recently, biphoton qutrits have been shown to improve the security and efficiency of quantum key distribution [8].

In the case of two qubits, there are four possible maximally entangled states, known as the Bell states. Vari-

ous photonic Bell state projections have been realized by using linear optics elements [beam-splitters, polarization beam-splitters (PBSs), and wave plates] [20, 21]. However, linear optics enables the simultaneous detection of only two of the four Bell states [22, 23]. A projection onto all four states has been demonstrated by a nonlinear interaction with low efficiency [24] and when hyperentanglement is present, by using the additional entangled degrees of freedom [25, 26]. Other demonstrations of full Bell state projection used auxiliary photons [27, 28] or path-entangled single photons [29].

Single photons can represent quantum systems of d states (qudits) by occupying d different modes [10–13]. The projection of two such photonic qudits of $d > 2$ onto a maximally entangled state is impossible without the use of auxiliary photons. This is because only two particles are involved, while the Schmidt number of the projected state is larger than 2 [30]. However, in the case of two biphoton qutrits, four particles are involved and a projection onto a maximally entangled qutrit state is possible.

In this Letter, we present an experimental scheme composed of linear optical elements that can project two biphoton qutrits onto a maximally entangled state. A generalized Bell basis of nine maximally entangled states is presented. We explicitly show that our scheme can discriminate one out of the nine states. A successful projection results in a coincidence detection of all four photons involved by single-photon detectors. Experimental results of such successful projections are presented.

We designate the three biphoton vectors whose amplitudes in Eq. 1 are α_0 , α_1 , and α_2 with the logical representation $|0\rangle$, $|1\rangle$ and $|2\rangle$, respectively. One possible way to write the maximally entangled basis of two qutrits is [3]

$$|\psi_{mn}\rangle = \frac{1}{\sqrt{3}} \sum_j \tau^{jn} |j\rangle_a \otimes |(j+m) \bmod 3\rangle_b, \quad (2)$$

where τ is defined as $e^{\frac{2\pi i}{3}}$ - the third root of unity - a and b are spatial modes, and the values of m , n , and j can

be 0, 1, and 2. From this general form, nine maximally entangled biphoton states can be explicitly written, arranged in three groups according to their m values,

$$\begin{aligned} |\psi_{0n}\rangle &= \frac{1}{\sqrt{12}}(a_h^\dagger{}^2 b_h^\dagger{}^2 + 2\tau^n a_h^\dagger a_v^\dagger b_h^\dagger b_v^\dagger + \tau^{2n} a_v^\dagger{}^2 b_v^\dagger{}^2)|\text{vac}\rangle, \\ |\psi_{1n}\rangle &= \frac{1}{\sqrt{6}}(a_h^\dagger{}^2 b_h^\dagger b_v^\dagger + \tau^n a_h^\dagger a_v^\dagger b_v^\dagger{}^2 + \frac{1}{\sqrt{2}}\tau^{2n} a_v^\dagger{}^2 b_h^\dagger{}^2)|\text{vac}\rangle, \\ |\psi_{2n}\rangle &= \frac{1}{\sqrt{6}}(\frac{1}{\sqrt{2}}a_h^\dagger{}^2 b_v^\dagger{}^2 + \tau^n a_h^\dagger a_v^\dagger b_h^\dagger{}^2 + \tau^{2n} a_v^\dagger{}^2 b_h^\dagger b_v^\dagger)|\text{vac}\rangle. \end{aligned} \quad (3)$$

The three groups differ from each other by permutations of the b mode vector. The three vectors of each group differ by the phase difference between their terms. Here we focus on the detection of states from the $|\psi_{0n}\rangle$ family.

If a certain configuration produces the qubit photonic Bell state $|\phi^+\rangle$ [1], its second-order process, i.e., when two photons of a single pulse split simultaneously, results in the state [31]

$$|\phi^{(2)}\rangle = \frac{1}{\sqrt{12}}(a_h^\dagger{}^2 b_h^\dagger{}^2 + 2e^{i\delta} a_h^\dagger a_v^\dagger b_h^\dagger b_v^\dagger + e^{2i\delta} a_v^\dagger{}^2 b_v^\dagger{}^2)|\text{vac}\rangle. \quad (4)$$

By tuning the angle δ , by using a birefringent crystal in one of the spatial modes, between $\delta = 0^\circ$, 120° , and 240° , it is possible to continuously change between the three states $|\psi_{00}\rangle$, $|\psi_{01}\rangle$, and $|\psi_{02}\rangle$, respectively.

In order to explain our projection scheme, we first examine the output of a PBS when each state of the three maximally entangled groups serves as its input. The first three states $|\psi_{0n}\rangle$ pass through the PBS without any change, up to a birefringent phase from the reflection of the vertically polarized photons. This phase can be compensated for either before or after the PBS. On the other hand, the remaining six states $|\psi_{1n}\rangle$ and $|\psi_{2n}\rangle$ are not preserved by the PBS operation. None of them results in a biphoton at each of the output ports. Thus, postselecting only cases when two photons exit from each of the PBS ports already discriminates between the three states of the first group and the six other states. In order to discriminate between the different members of the $|\psi_{0n}\rangle$ family and complete the projecting measurement, we add to the output of each of the PBS ports a half-wave plate at an angle θ with the vertical direction (see Fig. 1). Finally, the two polarizations of each mode are split by another PBS into two single-photon detectors. Regardless of the wave-plate angles, the first PBS certifies that a simultaneous fourfold detection at all of the detectors can originate only from states of the $|\psi_{0n}\rangle$ form. Propagating this general state through the presented setup results in nine different quantum amplitudes, one for each of the different options to have two photons at each of the two arms. The amplitude of the $a_h^\dagger a_v^\dagger b_h^\dagger b_v^\dagger$ term for fourfold detection can be simplified to

$$A_{4f} = \frac{1}{\sqrt{12}}(\sin^2 4\theta + 2\tau^n \cos^2 4\theta + \tau^{2n} \sin^2 4\theta). \quad (5)$$

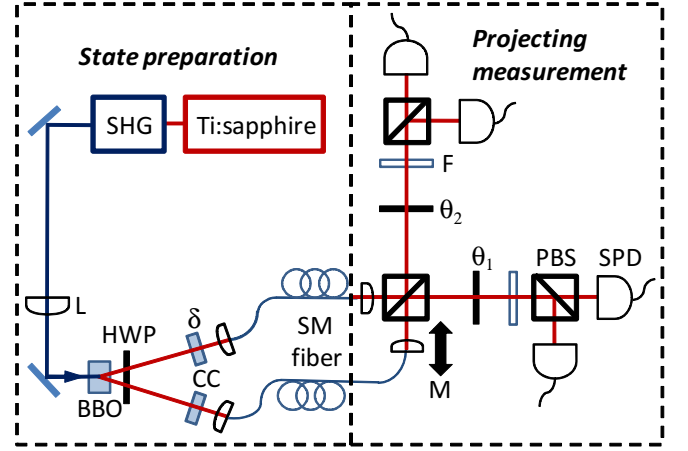


FIG. 1. (Color online) The experimental setup: a mode-locked Ti:sapphire laser at 780 nm is up-converted by second harmonic generation (SHG). The 230 mW beam is focused by a lens (L) on a 2 mm thick β -barium-borate (BBO) crystal, cut for the generation of polarization entangled photon pairs via type-II parametric down-conversion. The down-converted photons flip polarization at a half-wave plate (HWP) at 45° and temporal walk-off is corrected by compensating crystals (CC). One of the crystals is used to tune the birefringent angle δ [Eq. 4]. The photons are coupled into single mode fibers (SM) where their polarization is adjusted by polarization controllers. After the photons from both modes exit the fibers, they are overlapped at a polarization beam-splitter. The relative propagation delay between the two optical paths is adjusted by translating one of the fiber ends by a linear motor (M). The two half-wave plates at angles θ_1 and θ_2 are used to complete the projection process. After passing the projection configuration, the photons are spectrally filtered by using 3 nm wide bandpass filters (F) and coupled into multimode fibers that guide them to single-photon detectors (SPD).

The requirement that this amplitude should vanish when $n = 1$ and 2 is fulfilled when

$$\tan^2 4\theta = 2 \longrightarrow \theta \simeq 13.68^\circ. \quad (6)$$

This result can be generalized by allowing the two wave-plate angles to differ from each other. It can be shown that the condition for two independent wave-plate angles θ_1 and θ_2 is

$$\tan 4\theta_1 \tan 4\theta_2 = 2. \quad (7)$$

Nevertheless, the maximum theoretical fourfold coincidence rate is obtained in the degenerate case. Thus, by setting the angles of the two wave plates to 13.68° , fourfold coincidence can originate only from $|\psi_{00}\rangle$ with a detection probability of $\frac{1}{3}$. The probability is smaller than 1 as the $|\psi_{00}\rangle$ state can also result in quantum states other than $a_h^\dagger a_v^\dagger b_h^\dagger b_v^\dagger$. The source of those other states cannot be distinctively related to a single state, and thus their detection is useless for entanglement projection. The setup can be altered to detect the $|\psi_{01}\rangle$ or the $|\psi_{02}\rangle$ states as well, by adding a birefringent phase in

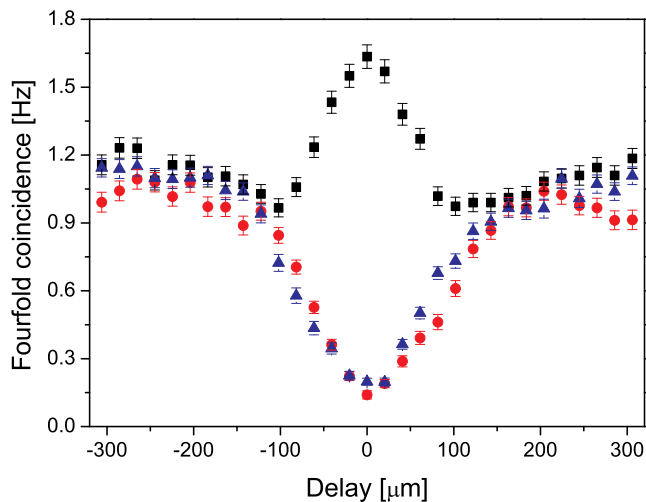


FIG. 2. (Color online) Experimental results of the fourfold coincidence rates as a function of the relative delay for the three $|\psi_{0n}\rangle$ states. Each data point was averaged over 600 seconds. The desired $|\psi_{00}\rangle$ state (black squares) shows a relative increase in the coincidence rate by about 50% at zero delay, when compared to large delays. The $|\psi_{01}\rangle$ (red circles) and $|\psi_{02}\rangle$ (blue triangles) states are well rejected, as shown by their considerable signal decrease at zero delay.

one arm before the PBS of -120° or -240° , respectively. Interestingly, the fourfold detection amplitude vanishes when one wave plate is at 0° and the other at 22.5° for all $|\psi_{0n}\rangle$ states. This parameter setting was recognized in a previous work in the context of nonlocal bunching [32].

The discussion until now assumed complete spatiotemporal overlap between the photons in spatial modes a and b . When the optical paths leading to the PBS differ, the photons in each mode are temporally labeled and therefore are distinguishable. The fourfold coincidence term $a_h^\dagger a_v^\dagger b_h^\dagger b_v^\dagger$ is split into six noninterfering terms. The expected fourfold coincidence detection probability for each of the three $|\psi_{0n}\rangle$ states becomes $\frac{2}{9}$. Thus, we expect all three states to have the same background rate when temporal distinguishability is introduced, as this is a projection onto a uniform mixture of these states. When distinguishability is removed, the rates from states $|\psi_{01}\rangle$ and $|\psi_{02}\rangle$ decrease to zero while the $|\psi_{00}\rangle$ rate would have a 50% increase over the background.

To demonstrate the suggested projection, we used the experimental setup shown in Fig. 1. When the half wave-plate angles θ_1 and θ_2 are both set at 22.5° , this setup becomes identical to a two qubits $|\phi^\pm\rangle$ projecting setup. We used this configuration to calibrate the birefringent angle δ as well as to find the zero delay position. A total rate of about 25000 twofold coincidences per second was observed with a dip visibility of $(95 \pm 1)\%$ (not presented here). The high twofold visibility figure indicates the quality of the PBS projection [33].

The states of the $|\psi_{1n}\rangle$ and $|\psi_{2n}\rangle$ families can not be generated by our setup. Nevertheless, their rejection is a result of the basic nature of PBSs. The PBS we have used has 5% reflection for a horizontally polarized beam, whereas an ideal PBS should have none. Using this figure, we calculated the probability to detect a state from these families to be around 1% in the worst possible case, when the input is a mixture of these families. Thus, we concentrate on demonstrating the discrimination between the three states of the $|\psi_{0n}\rangle$ family. Using the angle calibration, we tuned δ to be 0° , 120° , and 240° in order to produce the $|\psi_{00}\rangle$, $|\psi_{01}\rangle$, and $|\psi_{02}\rangle$ states, respectively. The wave-plate angles were tuned to 13.68° according to Eq. 6, and the delay between the paths was scanned. We present the results of these scans in Fig. 2. At the region of no temporal overlap (large delay), the three states share the same fourfold event background rate of 1.1 ± 0.1 Hz. When distinguishability is removed at the zero delay position, $|\psi_{00}\rangle$ shows a clear rise in the fourfold rate to a maximal value of 1.63 ± 0.05 Hz, while the orthogonal states $|\psi_{01}\rangle$ and $|\psi_{02}\rangle$ decrease to minimal values of 0.14 ± 0.02 and 0.19 ± 0.02 Hz, respectively. The background rates at zero delay for $|\psi_{01}\rangle$ and $|\psi_{02}\rangle$ are attributed to both imperfect initial state generation and the higher order term of six photons. The ratio between the projected and the rejected states is about 10, indicating a good projection fidelity. The ratio between the $|\psi_{00}\rangle$ signal values at zero delay and at large delay is ~ 1.5 , in accordance with the theoretical prediction up to experimental error. As the theoretical maximum efficiency of this projection is $\frac{1}{3}$, these rates indicate a combined production and detection rate of about 5 fourfold events per second.

As the birefringent angle δ is continuous, it is possible to generate not just the three $|\psi_{0n}\rangle$ states but a continuous range, as can be seen by Eq. 4. We set the delay position to zero, where projection occurs, and scanned this angle. The expected rate is $|A_{4f}|^2$ [Eq. 5], where we replaced the discrete variable n with a continuous phase $\delta = \frac{2\pi}{3}n$. The results of this measurement are shown in Fig. 3. Measurements for three wave-plate settings were performed. At $\theta = 0^\circ$ only the central term of the rate [Eq. 5] is nonzero, and thus when calculating $|A_{4f}|^2$, there is no interference between the three terms and the rate is independent of δ . When the wave plates' angle is $\theta = 22.5^\circ$, the central term is always zero and the first and last terms have identical magnitudes. These two terms interfere as $\cos^2 \delta$. The third wave-plate setting is at $\theta = 13.68^\circ$, where all three terms interfere with the same magnitude. As expected, this curve has a maximum value at $\delta = 0^\circ$ (corresponding to the $|\psi_{00}\rangle$ state) and two minima at $\delta = 120^\circ$ and 240° , when the states $|\psi_{01}\rangle$ and $|\psi_{02}\rangle$ are generated. The experimental data fit the predicted theoretical curves well. The visibilities of the $\theta = 22.5^\circ$ and $\theta = 13.68^\circ$ curves are 0.77 ± 0.1 and 0.82 ± 0.04 , respectively. Deviations (most apparent

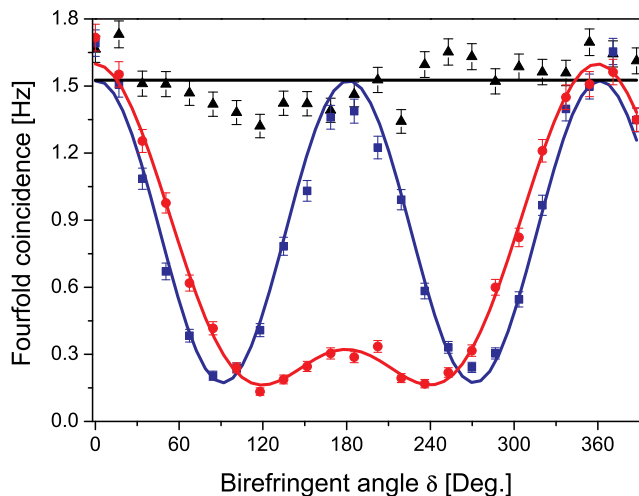


FIG. 3. (Color online) Experimental results of the fourfold coincidence rates as a function of the birefringent angle δ for three wave-plate angle settings: $\theta = 0^\circ$ (black triangles), $\theta = 22.5^\circ$ (blue squares) and $\theta = 13.68^\circ$ (red circles). Each data point was averaged over 480 seconds. The solid lines represent the fit to theoretical predictions.

in the $\theta = 0^\circ$ data) are mainly due to laser power and coupling fluctuations during the long overall acquisition time of about 11 hours.

A quantum communication network with qutrits will provide many advantages that were suggested in previous works [8, 16–19]. For such a network to be practical, qutrit quantum repeaters should be available. These future devices are based on entanglement swapping which in turn relies on projection onto maximally entangled states. As mentioned above, it is impossible to realize such a projection with linear operations on qutrits that are represented by single photons [30]. This fact rules out as practical candidates most of the qutrit realizations to date. Polarized biphotons are a clear exception to this, as is shown by this work.

In a recent work, two photons from two different entangled pairs have been projected onto the symmetric triplet subspace of biphotons [34]. This projection created a qubit-qutrit-qubit chain, which is a valence-bond solid ground state [35]. However, since the projection involves only two single photons, it is equivalent to the standard qubit Bell measurement [2].

In conclusion, we have demonstrated a linear optics scheme that projects two biphoton qutrits onto a maximally entangled state. Three such orthogonal states were prepared and the scheme's ability to discriminate between them has been shown. When a continuous phase between these states was scanned, the output fourfold signal has been shown to fit the theoretical prediction very well. The demonstration of qutrit teleportation us-

ing this projection is currently under progress.

The authors thank the Israeli Science Foundation for supporting this work under Grants No. 366/06 and No. 546/10.

-
- [1] P.G. Kwiat *et al.*, Phys. Rev. Lett. **75**, 4337 (1995).
 - [2] H. Weinfurter, Europhys. Lett. **25**, 559 (1994).
 - [3] C.H. Bennett *et al.*, Phys. Rev. Lett. **70**, 1895 (1993).
 - [4] D. Bouwmeester *et al.*, Nature (London) **390**, 575 (1997).
 - [5] J.-W. Pan, D. Bouwmeester, H. Weinfurter and A. Zeilinger, Phys. Rev. Lett. **80**, 3891 (1998).
 - [6] H.-J. Briegel, W. Dür, J.I. Cirac and P. Zoller, Phys. Rev. Lett. **81**, 5932 (1998).
 - [7] A.V. Burlakov *et al.*, Phys. Rev. A **60**, R4209 (1999).
 - [8] I. Bregman, D. Aharonov, M. Ben-Or and H.S. Eisenberg, Phys. Rev. A **77**, 050301 (2008).
 - [9] B.P. Lanyon *et al.*, Phys. Rev. Lett. **100**, 060504 (2008).
 - [10] A. Mair, A. Vaziri, G. Weihs and A. Zeilinger, Nature (London) **412**, 313 (2001).
 - [11] S. Gröblacher *et al.*, New J. of Phys. **8**, 75 (2006).
 - [12] L. Bartůšková *et al.*, Phys. Rev. A **74**, 022325 (2006).
 - [13] R.T. Thew, A. Acín, H. Zbinden and N. Gisin, Phys. Rev. Lett. **93**, 010503 (2004).
 - [14] M. Reck, A. Zeilinger, H. J. Bernstein, and P. Bertani, Phys. Rev. Lett. **73**, 58 (1994).
 - [15] Q. Lin and B. He, Phys. Rev. A **80**, 062312 (2009).
 - [16] M. Fitzi, N. Gisin and U. Maurer, Phys. Rev. Lett. **87**, 217901 (2001).
 - [17] A. Cabello, Phys. Rev. Lett. **89**, 100402 (2002).
 - [18] Č. Brukner, M. Żukowski and A. Zeilinger, Phys. Rev. Lett. **89**, 197901 (2002).
 - [19] N.K. Langford *et al.*, Phys. Rev. Lett. **93**, 053601 (2004).
 - [20] K. Mattle, H. Weinfurter, P.G. Kwiat and A. Zeilinger, Phys. Rev. Lett. **76**, 4656 (1996).
 - [21] G. Di Giuseppe, F. De Martini and D. Boschi, Phys. Rev. A **56**, 176 (1997).
 - [22] L. Vaidman and N. Yoran, Phys. Rev. A **59**, 116 (1999).
 - [23] N. Lütkenhaus, J. Calsamiglia and K.-A. Suominen, Phys. Rev. A **59**, 3295 (1999).
 - [24] Y.H. Kim, S.P. Kulik and Y. Shih, Phys. Rev. Lett. **86**, 1370 (2001).
 - [25] P.G. Kwiat and H. Weinfurter, Phys. Rev. A **58**, R2623 (1998).
 - [26] C. Schuck, G. Huber, C. Kurtsiefer and H. Weinfurter, Phys. Rev. Lett. **96**, 190501 (2006).
 - [27] Z. Zhao *et al.*, Phys. Rev. Lett. **94**, 030501 (2005).
 - [28] P. Walther and A. Zeilinger, Phys. Rev. A **72**, 010302(R) (2005).
 - [29] D. Boschi *et al.*, Phys. Rev. Lett. **80**, 1121 (1998).
 - [30] J. Calsamiglia, Phys. Rev. A **65**, 030301(R) (2002).
 - [31] A. Lamas-Linares, J.C. Howell and D. Bouwmeester, Nature (London) **412**, 887 (2001).
 - [32] H.S. Eisenberg, J.F. Hodelin, G. Khoury and D. Bouwmeester, Phys. Rev. Lett. **94**, 090502 (2005).
 - [33] H.S. Poh *et al.*, Phys. Rev. A **80**, 043815 (2009).
 - [34] R. Kaltenbaek *et al.*, Nat. Phys. (London) **6**, 850 (2010).
 - [35] A.S. Darmawan and S.D. Bartlett, Phys. Rev. A **82**, 012328 (2010).